

# **Modifications of a Sinarback 54 Digital Camera for Spectral and High-Accuracy Colorimetric Imaging: Simulations and Experiments**

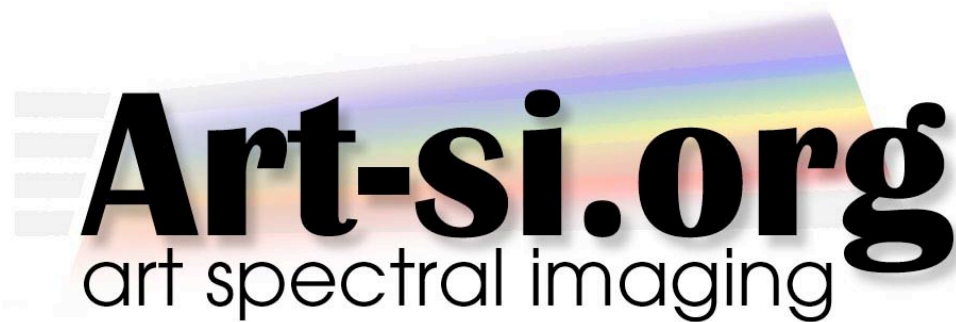
**Roy S. Berns**

**Lawrence A. Taplin**

**Mahdi Nezamabadi**

**Yonghue Zhao**

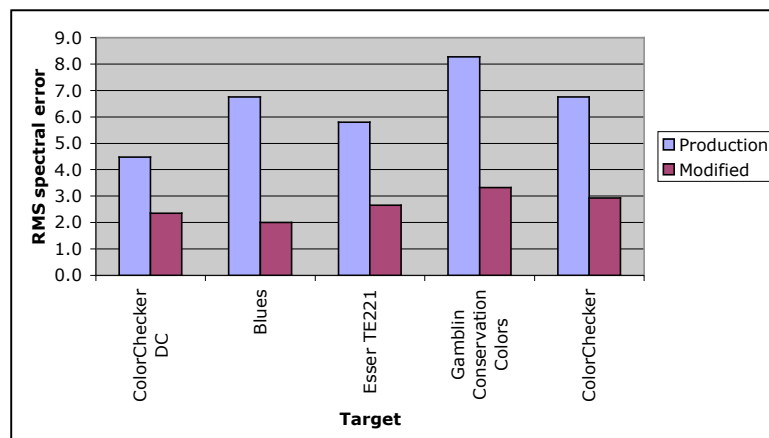
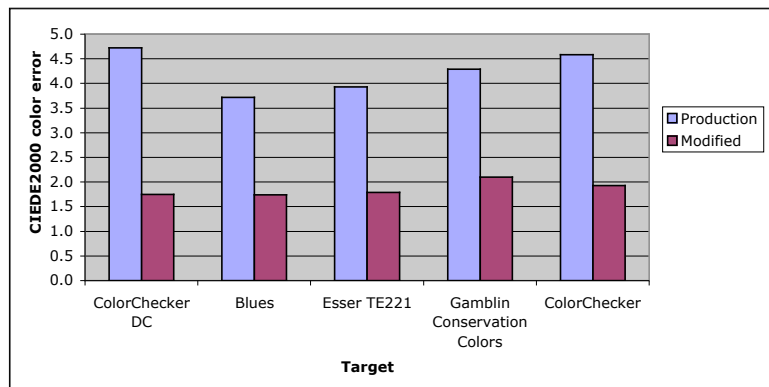
**Munsell Color Science Laboratory  
Chester F. Carlson Center for Imaging Science  
Rochester Institute of Technology**



**June, 2004**

## I. Executive Summary

A search technique was used to identify sets of colored glass filters that could be placed in the optical path of the Sinarback 54 camera system resulting in improved color accuracy compared with a production unit and the ability to perform spectral estimation. A green and blue filter, each a pair of filters, were identified and constructed from Schott glass. RGB images were collected through these two filters resulting in six image planes. Using the Gretag Macbeth ColorChecker DC and a custom target of blue artist pigments, a transformation was derived that converted digitally flat-fielded and photometrically-linearized camera signals to estimated spectral reflectance factor. The combination of using these two filter “sandwiches” and appropriate mathematics resulted in more than a twofold improvement in color and spectral accuracy compared with the production camera. The average colorimetric and spectral performance is shown in the following bar graphs for the calibration targets and independent-verification targets, the Esser TE221 test chart, a custom target of artist pigments made using the Gamblin Conservation Colors, and the traditional GretagMacbeth ColorChecker Color Rendition chart. These results indicate that it is possible to achieve excellent color accuracy and acceptable spectral accuracy using a color-filter array sensor.



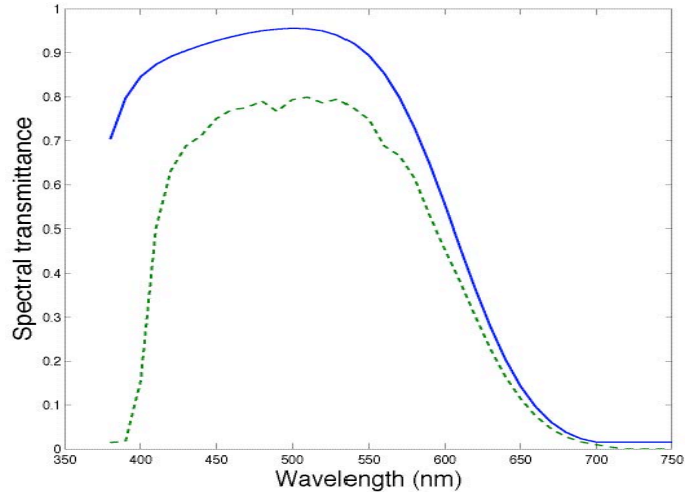
## II. Introduction

At the Munsell Color Science Laboratory (MCSL), we have an extensive research program in spectral-based color reproduction including capture, archiving, and printing. In image capture, we have evaluated full spectral methods where 31 or more image planes are acquired as well as two abridged methods. The first abridged method uses a monochrome sensor and six absorption filters. The six image planes are captured sequentially. The second abridged method uses a color-filter array (CFA) camera and one or more absorption filters. The basic idea is to capture sets of RGB images, each set using a colored filter. The experiment described in this report was limited to two sets of RGB images, that is, six total images. By imaging test targets with known spectral reflectance factor, a transformation is developed that converts the six image planes to a multi-plane spectral image, i.e., 380 – 750 nm in 10 nm increments resulting in 41 image planes. These spectral images can be rendered for a specific CIE illuminant and observer pair. This is an abridged method because only six images are collected and a full spectral image is estimated mathematically.

During the 2002 and 2003 academic years, we have been active in applying our multi-filter technique for use with CFA digital cameras, described at [www.Art-SI.org](http://www.Art-SI.org), an abbreviation for Art Spectral Imaging. During the 2002 academic year, a MS thesis was performed by David Collin Day that used Wratten filters and Kodak's KAF-16802CE CFA. During the 2003 academic year we have been performing extensive simulations using the nominal spectral sensitivities of Kodak's KAF-22000CE CFA. This sensor is used with the Sinarback 54. Also during the 2003 academic year, we purchased a Sinarback 54 as well as complementary camera optics and Broncolor lighting systems. During June, 2004, we tested our multi-filter approach using the Sinarback 54. This testing included a comparison between simulated and actual camera signals, and the performance of several sets of candidate filters. This technical report will describe this testing, focusing on the set of filters yielding the best performance.

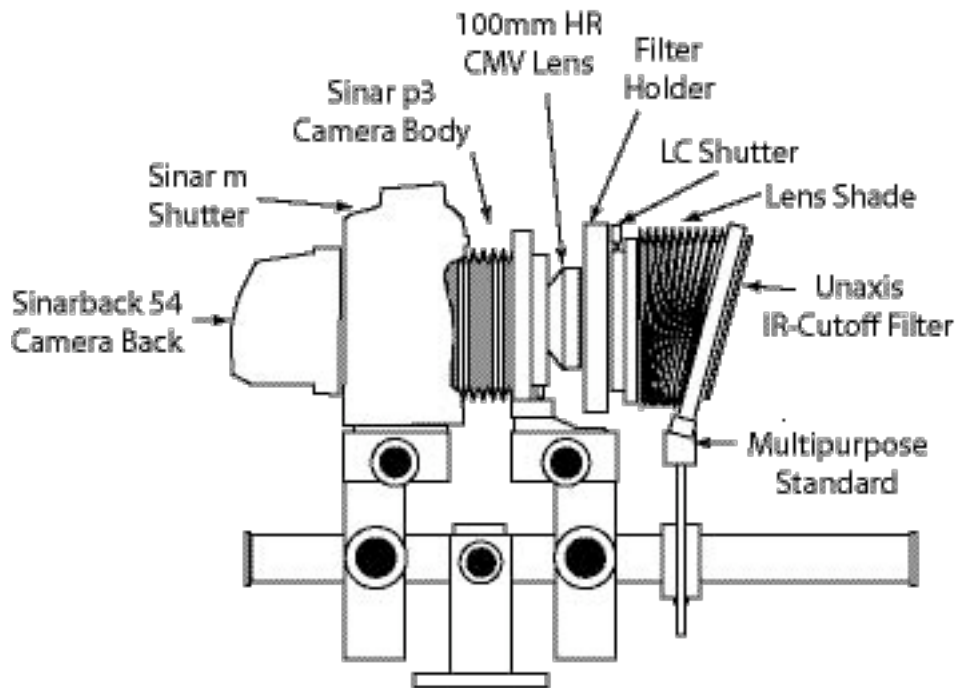
## III. Sinarback 54 Digital Camera

The Sinarback 54 digital camera is a three channel digital camera that uses a Kodak KAF-22000CE CCD with a resolution of 5440 x 4880 pixels. This sensor is a Bayer-pattern CFA. The camera has a built-in IR cut-off filter, which was removed and replaced with clear BK7 glass. In front of the camera lens, a Unaxis visible-spectrum bandpass filter was used. This increased the range of wavelength sensitivity compared with Sinar's IR filter. With our modified camera we sought to simulate the "stock" Sinarback by imaging through a Schott BG39 glass filter with thickness of 3 mm. (We just happened to have a BG39 at this thickness.) Figure 1 presents the spectral transmittance of the standard Sinar IR cut-off filter and its replacement for our experiments, the combination of the Unaxis and BG39 filters.



**Figure 1.** Spectral transmittance of IR cut-off filters in Sinarback 54 camera; solid line is built-in IR cut-off filter in the fabricated camera; dashed line is combined transmittance of Unaxis IR cut-off filter and Schott BG39 glass filter.

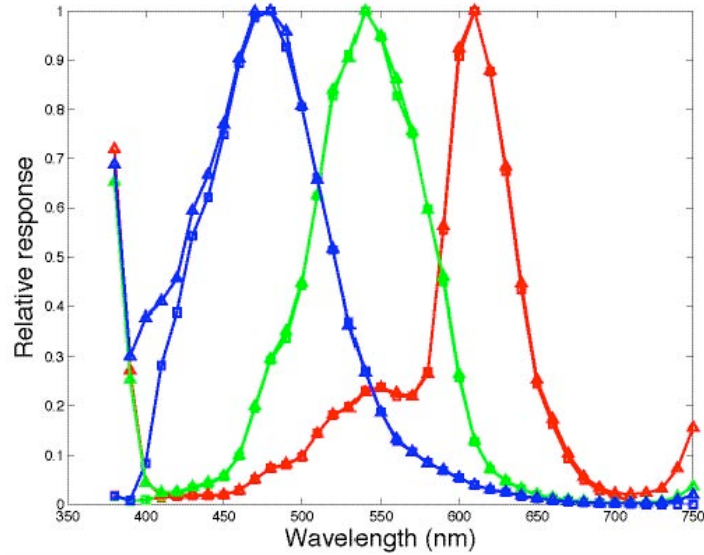
A schematic of the Sinarback and associated optics is shown in Figure 2. The Unaxis filter was placed at the end of the lens shade. The shade was angled to prevent inter-reflections between the filter and lens. The filter holder was fabricated using black foamcore.



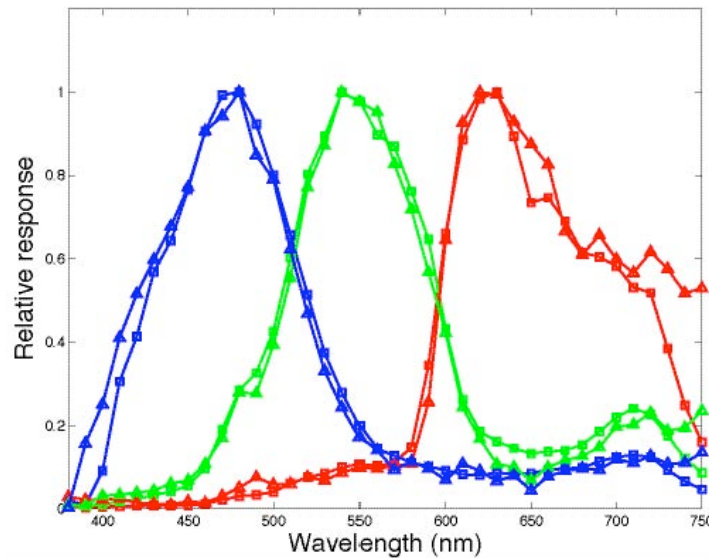
**Figure 2.** Schematic of the Sinar camera system used in these experiments.

Figure 3 shows measured spectral sensitivities of the camera modulated by the original and replacement filters. As it can be seen, the original built-in IR cut-off and its replacement counterpart has the same effect on camera spectral sensitivity except for the blue channel in wavelengths lower than 430 nm. At the beginning of this research, the Sinarback 54 was not available at our lab; hence filter

optimization was simulated based on nominal spectral sensitivities of the camera. Camera spectral sensitivity was later measured using a calibrated spectroradiometer (Photo Research SpectraScan PR650) and a light source coupled with a monochromator. The similarity between the nominal and measured spectral sensitivities are shown in Figure 4. The similarity is reasonable except towards the long-wavelength portion of the visible spectrum.



**Figure 3.** Normalized spectral sensitivity of camera combined with IR cut-off filter; solid line with triangle is camera sensitivity combined with built in IR cut-off filter; solid line with square is camera sensitivity combined with Unaxis IR cut-off filter and Schott BG39 filter with 3 mm thickness.



**Figure 4.** Normalized spectral camera sensitivity; solid line with square is measured camera sensitivity; solid line with triangle is nominal camera spectral sensitivity.

## IV. Calibration Targets and Lightings

There are several common targets available for system calibration, for example, the GretagMacbeth ColorChecker DC (CCDC), the GretagMacbeth ColorChecker Rendition Chart (CC), and the Esser Test Chart TE221 (Esser). These calibration targets have 240, 24, and 283 samples, respectively. These targets were designed with different criteria than those required for spectral estimation. For example, the range of pigmentation of the CCDC is limited, particularly for blues. In much of our research performed previously [1], a separate target of 56 blues using artist acrylic paints including cobalt blue and ultramarine blue were used as a calibration target along with the CCDC. A similar target was used in this research. Furthermore some samples were made of typical artist's pigments using the Gamblin Conservation Colors and were used in this research. All the targets were measured using an integrating sphere spectrophotometer, specular component excluded.

The Broncolor HMI F1200, manufactured by Bron Elektronik AG was used in this research. Figure 5 shows relative spectral power distribution of this lighting.

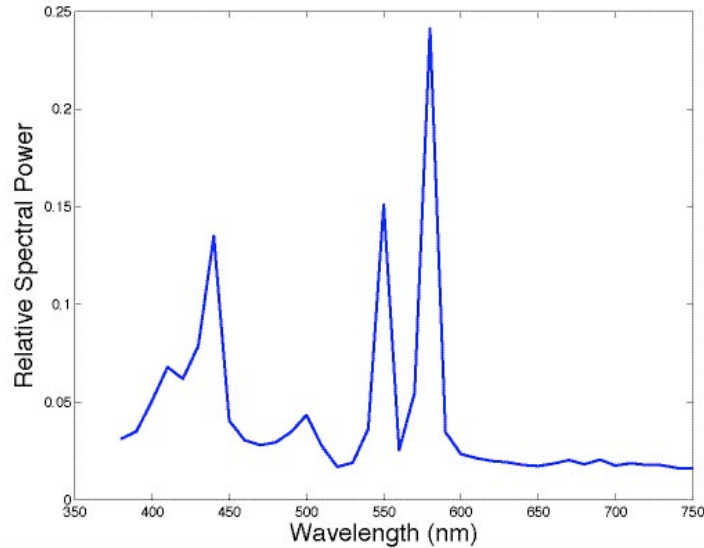


**Figure 5.** Relative spectral power distribution of Broncolor HMI F1200 lighting. Measurements were made using a PhotoResearch PR704.

## V. Virtual Camera Model

In the first part of the simulation phase, the nominal spectral sensitivities of the camera were used. The spectral sensitivity of the camera system is the product of the sensor response, and any filtering elements between it and the subject, in this case, the glass absorption and IR cut-off filters were considered. (For this analysis, the lens transmittance was ignored.) We denote the combined spectral sensitivity by  $\mathbf{S}_{\lambda,i}$ , as shown in equation (1):

$$\mathbf{S}_{\lambda,i} = F_{\lambda} \cdot I_{\lambda} \cdot \mathbf{C}_{\lambda,i} \quad (1)$$

where  $\lambda$  is wavelength, ranging from 380 (nm) to 750 (nm) at 10 (nm) intervals,  $\mathbf{C}_{\lambda,i}$  is the spectral response of camera for the  $i$ th channel at each wavelength,  $I_{\lambda}$  and  $F_{\lambda}$  are spectral transmittances of IR cut-off and glass filters, respectively, and  $\mathbf{S}_{\lambda,i}$  is the resulting spectral sensitivity for the entire camera

system.

The digital counts for a pixel responding to a sample of known reflectance factor can be computed using equation (2):

$$\mathbf{D}_i = \sum_{\lambda=380}^{750} (\mathbf{R}_\lambda \cdot \mathbf{L}_\lambda \cdot \mathbf{S}_{\lambda,i}) + n_i \quad (2)$$

where  $\lambda$  is wavelength, ranging from 380 (nm) to 750 (nm) at 10 (nm) intervals,  $D_i$  is the digital count of the  $i$ th channel,  $R_\lambda$  is the spectral reflectance factor of a pixel and  $L_\lambda$  is the relative spectral power distribution of the illuminant. A noise term,  $n_i$ , can be added to each channel. In the first stage of the simulation the noise term was set to zero to simplify the model. In the later stages, after reducing the total number of filters to a computationally feasible number, it was assumed to have a normal distribution with zero mean and a signal dependent standard deviation. The real camera system contains a 14-bit analog to digital converter (ADC), the filter selection simulation was carried out quantizing the signal to 12-bits; this difference should not significantly affect on the results. The simulation exposure time was set to prevent clipping of a perfect white diffuser. Maximum digital counts were set to 93% of the total range to allow room for highlights, as is our practice for the real camera. For each color calibration target a generalized pseudo inverse based on Singular Value Decomposition was used to generate a transformation matrix,  $\mathbf{T}$ , for converting digital counts to reflectance values as shown in equation (3):

$$\mathbf{T} = \mathbf{R} \cdot \text{PINV}(\mathbf{D}) \quad (3)$$

where  $\mathbf{R}$  is the matrix of reflectance factors of calibration samples,  $\text{PINV}$  is the Matlab pseudoinverse function and  $\mathbf{D}$  is the corresponding digital counts of the calibration samples. Knowing the transformation matrix and a set of digital counts, one can calculate estimated reflectance factor values according to equation (4) for that set of digital counts:

$$\hat{\mathbf{R}} = \mathbf{T} \cdot \mathbf{D} \quad (4)$$

where  $\hat{\mathbf{R}}$  is the estimated reflectance value matrix,  $\mathbf{D}$  is the digital count matrix, and  $\mathbf{T}$  is the transformation matrix. Spectral and colorimetric performance metrics can be constructed based on original and estimated reflectance factors. The goal of this research was to select the best combination of glass filters that yielded the highest spectral and colorimetric performance.

## VI. Glass Filter Selection

Sandwiches of glass filters were theoretically constructed by selecting two filters at a time from a pool of 41 Schott glass filters. The total thickness of each sandwich was restricted to 4mm and the thickness of each selected filter was 1 mm, 2 mm or 3 mm. In other words, the sandwiches could consist of two filters, a 1 mm and a 3 mm, or two filters of 2 mm. The case of a single 4 mm filter was also considered. Figure 6 presents the transmittance values of the 41 Schott glass filters with nominal 1 mm thicknesses. The transmittance of the filters at the other thicknesses was computed using Beer's law and sandwiched filters were assumed to be cemented together.

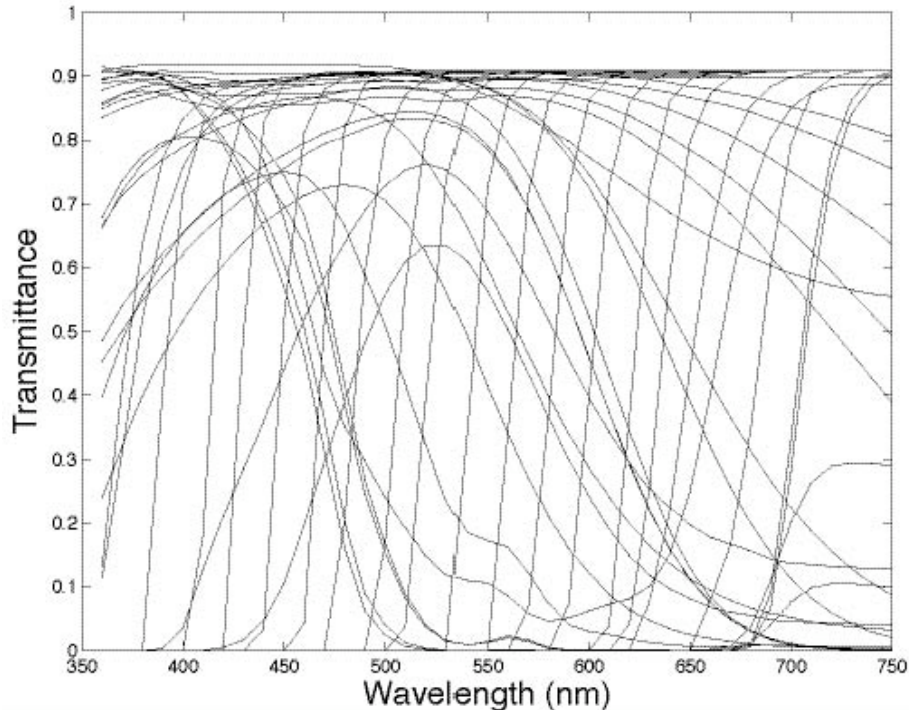


**Figure 6.** Transmittance of 41 Schott glass filters (1 mm thickness) used in generation of theoretical filters.

To avoid very low signal outputs, all combinations with average transmittance of less than 10% were discarded from further analysis. In this way 2380 theoretical filters were generated and stored as a new database of filters. In the next step different combinations of two filters were made from the theoretical database, which was 2,831,010 combinations. The Sinarback 54 has three color channels, but by placing two filters sequentially in front of the camera a system with 6 channels is created. The new system produces 6 digital counts per pixel, 3 for each filter. At this stage in the filter selection the noise term presented in equation (2) was set to zeros (noiseless camera model) and corresponding camera signals for the Esser and Gamblin targets were predicted for all two million filter -pair combinations. Then the associated transformation matrix,  $\mathbf{T}$ , for each filter combination was computed using Equation (3) and the digital counts of the Esser target. Estimated reflectance values for both the Esser calibration data and the independent Gamblin target were calculated using Equation (4) for the corresponding filter pairs. Based on estimated and original reflectance values for each target, the spectral and colorimetric accuracy metrics for each filter pair were calculated. Those filter pairs with performance lower than a threshold were eliminated. Furthermore, for those pairs that were sandwiches of the same type of filters but with different thicknesses, only the pair with the best performance was kept. Spectral RMS error was used to select the 30,000 filters with the highest spectral estimation accuracy.

In order to more accurately simulate the real camera system, noise must be taken into account. For the selected 30,000 pairs, noise was added to fifty simulated pixels per color sample. The noise term values were normally distributed, had a mean of zero and a standard deviation of 2.5% of the sample signal. Using Equation (4) and the noisy digital counts, the estimated reflectance values for the Esser target were recomputed. The spectral and colorimetric accuracy metrics were then calculated based on the new estimates and the measured reflectance values of the Esser target. Furthermore, the  $\mu$ -factor for the system spectral sensitivity associated with each filter pair was computed.  $\mu$ -factor is a metric that measures the similarities of the spectral sensitivities of a system to color matching functions (spectral

sensitivity of eye) [2]. A  $\mu$ -factor equal to unity indicates perfect correlation between spectral sensitivity of the imaging system and color matching functions. Conversely, a  $\mu$ -factor of zero means no similarity between spectral sensitivity of the imaging system and color matching functions. The  $\mu$ -factors presented here are the mean of CIE D65 as the taking illuminant, CIE A as the viewing illuminant and vice versa. Figures 7 and 8 show the relationship between  $\mu$ -factor values and spectral and colorimetric accuracy metrics. These metrics are based on the reconstruction of the Esser target and a data point is included for each of the selected 30,000 filter pairs.

Filter throughput affects the required exposure time and corresponding signal to noise ratio. Therefore, the sum of all six channels signals was also considered as a selection criterion. Figure 9 presents the spectral error metric versus the sum of output signals for each filter pair in estimation of the Esser calibration target.

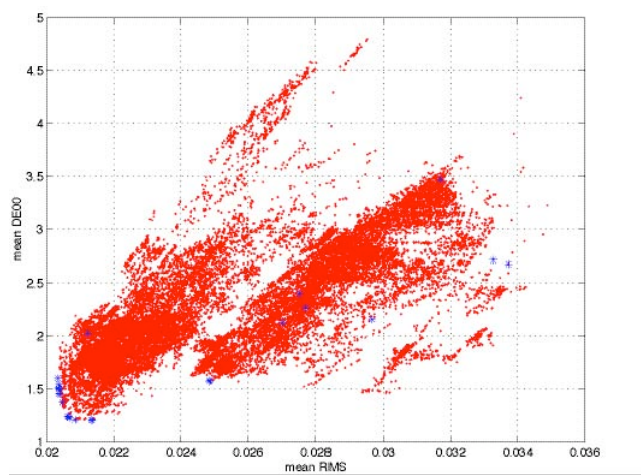


**Figure 7.** Mean color differences ( $\Delta E_{00}$  for D65), versus spectral error, RMS, in estimation of Esser calibration target for the selected 30,000 filter pairs. Blue asterisks mark 25 filter pairs selected for further analysis.

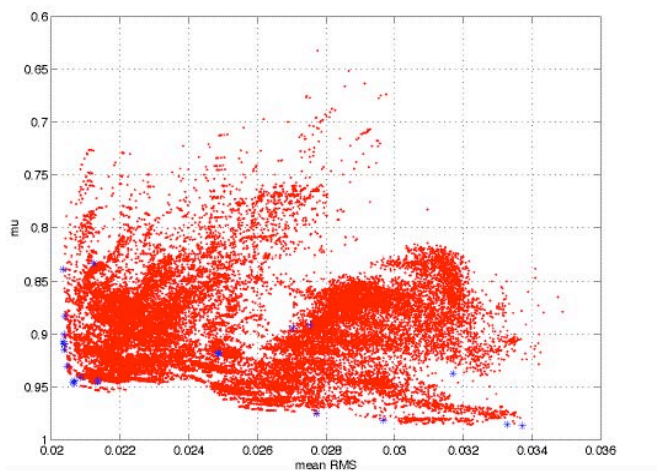


**Figure 8.** The  $\mu$ -factor values versus mean of RMS error in estimation of Esser calibration target for the selected 30,000 filter pairs. The same 25 filter pairs are marked by asterisk symbols as in Figure 7.

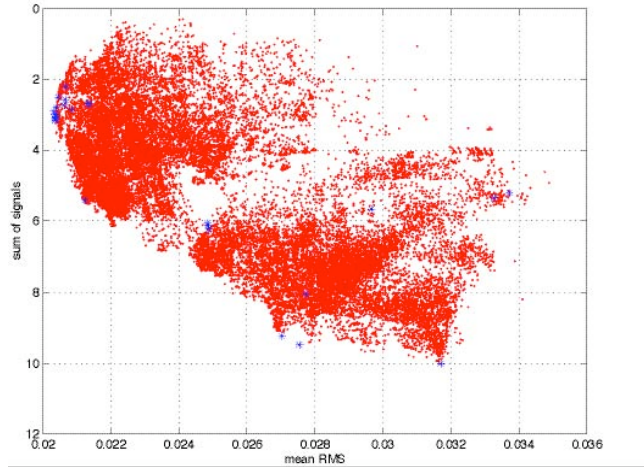
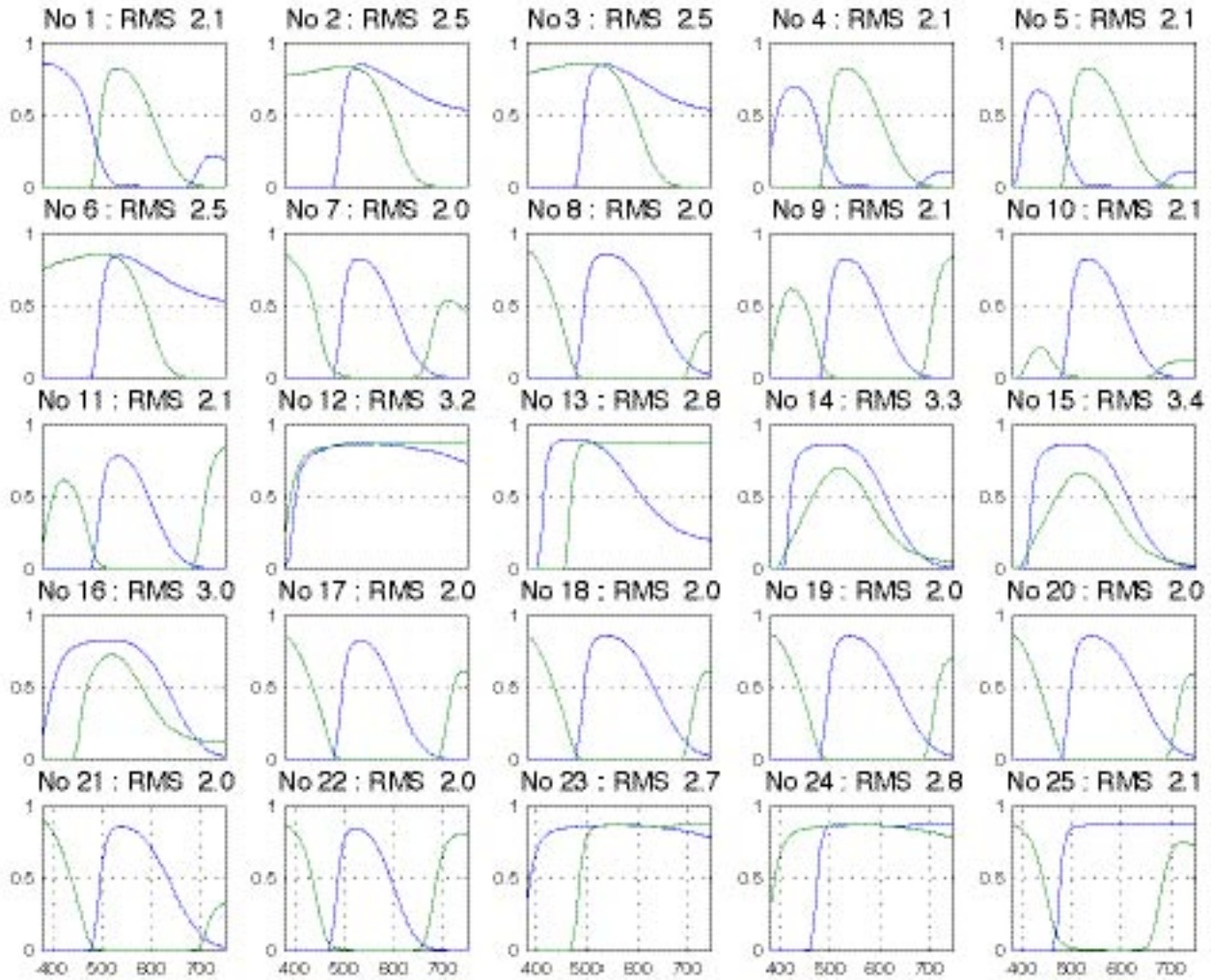


**Figure 9.** Sum of six channel signals versus mean of RMS error in estimation of Esser calibration target for the selected 30,000 filter pairs. A selection of 25 filter pairs is marked by asterisk symbols.

The ideal filter pair would have minimum spectral and colorimetric error ( $RMS=0$  and  $\Delta E_{00}=0$ ),  $\mu$ -factor equal to 1 and a high through put (large signal values). It was attempted to find a group of filters with these characteristics, Table I presents 25 selected filter pairs and their corresponding accuracy metrics and  $\mu$  factors. The selected filters are marked with asterisks in Figures 7 to 11. Figure 12 shows the spectral transmittance of the 25 pairs.

**Table I.** Spectral and colorimetric ( $\Delta E_{00}$  for D65) accuracies in estimation of Esser calibration target and  $\mu$ -factor values for 25 selected filter pairs. The  $\mu$ -factors are the mean for D65 as the taking illuminant, illuminant A as the viewing illuminant and vice versa.

No	Filter 1		Filter 2		Mean RMS%	Mean DE00	Max DE00	MU factor
	f11	f12	f21	f22				
1	BG25	KG4	BG39	GG495	2.1	1.2	7.4	0.941
2	BG26	GG495	BG40	KG3	2.5	1.6	8.7	0.918
3	BG26	GG495	BG40	KG4	2.5	1.6	9.2	0.918
4	BG12	GG385	BG39	GG495	2.1	1.2	6.7	0.944
5	BG12	GG400	BG39	GG495	2.1	1.2	6.9	0.945
6	BG26	GG495	BG40	BG40	2.5	1.6	8.9	0.917
7	BG39	GG495	BG24A	KG3	2.0	1.5	7.3	0.882
8	BG40	GG495	BG26	BG3	2.0	1.5	7.6	0.914
9	BG39	GG495	BG4	GG395	2.1	1.2	6.1	0.945
10	BG39	GG495	BG24A	VG6	2.1	1.2	6.5	0.943
11	BG18	GG495	BG4	GG395	2.1	1.2	6.8	0.946
12	GG400	KG2	GG385	GG385	3.2	3.5	13.1	0.937
13	BG26	GG420	GG400	GG475	2.8	2.3	12.7	0.975
14	BG38	GG420	KG1	VG6	3.3	2.7	12.0	0.985
15	BG38	GG420	KG3	VG6	3.4	2.7	12.3	0.987
16	BG40	GG395	GG455	VG6	3.0	2.2	11.2	0.981
17	BG39	GG495	BG3	KG2	2.1	1.4	6.5	0.930
18	BG40	GG495	BG3	KG2	2.0	1.5	8.8	0.909
19	BG40	GG495	BG3	KG4	2.0	1.5	8.3	0.909
20	BG40	GG495	BG4	KG2	2.0	1.5	7.9	0.900
21	BG40	GG495	BG26	BG4	2.0	1.5	8.4	0.907
22	BG40	GG495	BG24A	BG24A	2.0	1.6	9.2	0.838
23	GG385	KG4	GG420	GG495	2.7	2.1	10.4	0.894
24	GG420	GG475	GG385	KG4	2.8	2.4	13.2	0.891
25	GG395	GG475	BG24A	KG4	2.1	2.0	9.6	0.833



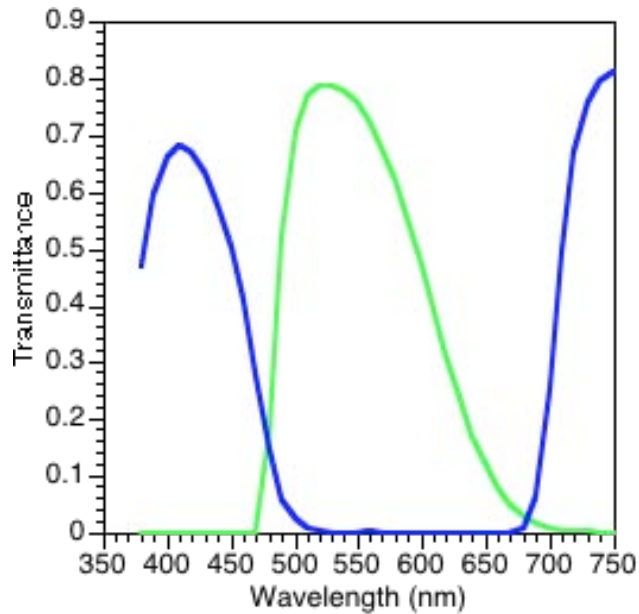
**Figure 12.** Spectral transmittance of 25 selected filter pairs. The spectral RMS error expressed as a percentage associated with estimation of the Esser calibration target is shown above of each graph next to the filter pair number. As indicated in the text, filter pairs 9 and 2 were selected and named Set A and Set B.

Figure 12 shows the similarity in transmittance and spectral RMS error for several groups of filters (for example pairs 2, 3 and 6). Colorimetric and spectral accuracy,  $\mu$ -factor and past experience were used to ultimately select filter pairs No. 9 and No. 2 for experimental testing. These filter pairs were named set A and set B, respectively. This report will be limited to set A since its performance was superior to set B. Table II shows predicted  $\mu$ -factors for different lightings situations using filter set A.

**Table II.** Calculated  $\mu$  factor values based on measured camera spectral sensitivity combined with Unaxis IR cut-off filter and filter set A using different illuminants.

		Filter set A (#9)			
		Viewing illuminants			
		D65	D50	A	HMI
Taking Illuminants	D65	0.941	0.946	0.958	0.486
	D50	0.944	0.950	0.962	0.484
	A	0.945	0.949	0.965	0.471
	HMI	0.758	0.758	0.771	0.851

The spectral transmittances of filter set A are plotted in Figure 13. One filter is green and the other is blue. The blue filter transmits both short- and long-wavelength visible radiation. The resulting spectral sensitivities for filter set A are plotted in Figure 14. The green filter is shaping the blue and red channels. The blue filter is shaping the blue channel and creating two long-wavelength channels from the green and red channels. Figure 15 shows a plot of all six channels normalized to unity peak height. We see how filter set A results in channels sampling the complete visible spectrum. In this manner, a color digital camera becomes a spectral imaging device.



**Figure 13.** Spectral transmittances of filter set A.

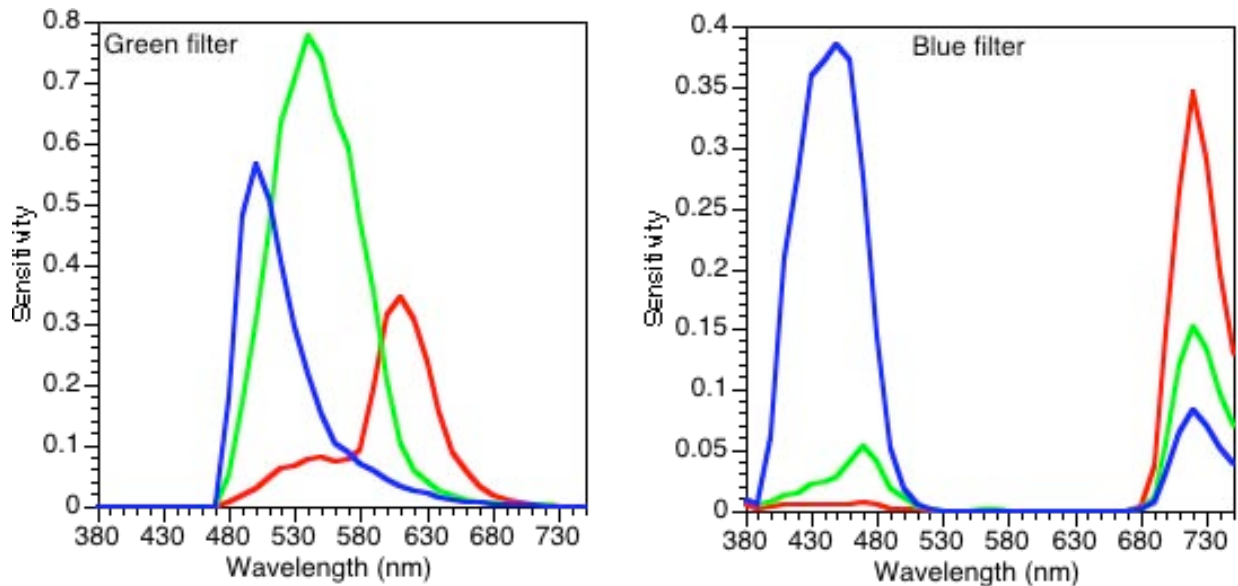


**Figure 14.** Spectral sensitivities of filter set A based on the nominal spectral sensitivities of the Sinarback 54 and the Unaxis filter.

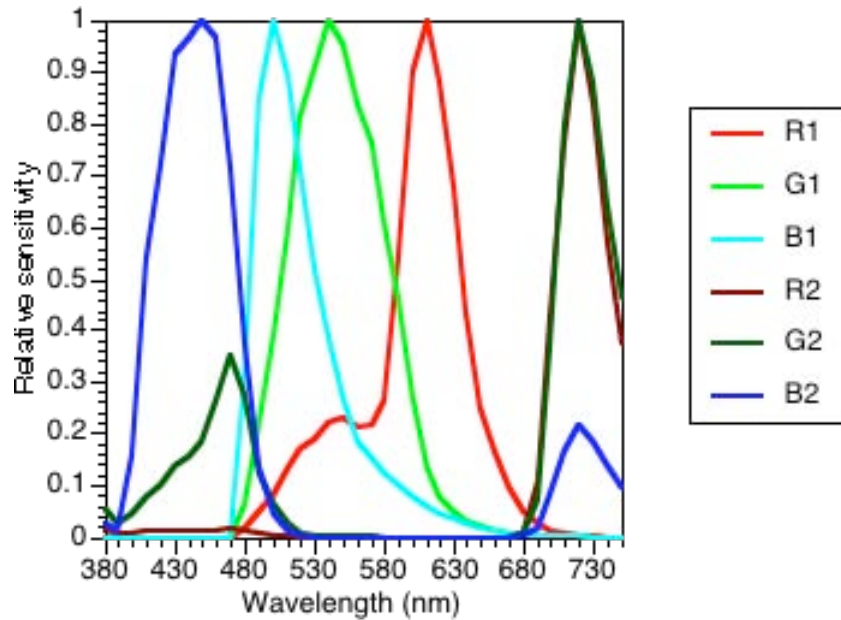


**Figure 15.** Peak-height normalized spectral sensitivities of modified Sinarback 54 and filter set A.

Selecting filter set A was based on evaluating both spectral and colorimetric accuracy. Thus, we can evaluate the similarity of the six channels, when combined linearly, to CIE color matching functions. Filter set A and the our simulation of the production Sinarback 54 (using the BG39) are compared in Figure 16. The modified Sinarback has spectral sensitivities much closer to color matching functions than the production camera. The improvement in  $\bar{z}$  is notable.

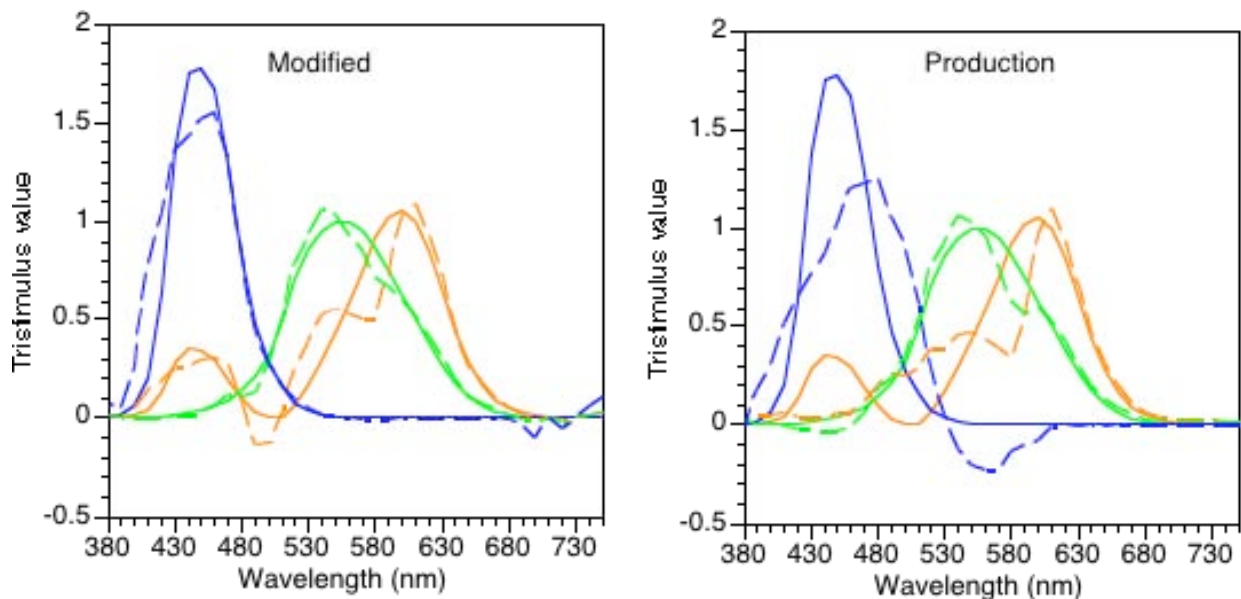


**Figure 16.** Comparison between modified (filter set A) and production Sinarback 54 in fitting the 1931 standard observer color matching functions. Solid lines are the CIE color matching functions; dashed lines are their fit: blue represents  $\bar{z}$ , green represents  $\bar{y}$ , and orange represents  $\bar{x}$ .

## VII. Experimental

The Schott glass comprising filter set A was purchased and formed into the blue and green “sandwiches.” Since we had yet to determine how well our virtual camera model performed, we did not cement the filters together. For each scene, we took an image using the filter set A green, the filter set A blue, and the BG39. In all cases we included the Unaxis visible radiation bandpass filter. Two Broncolor HMI lights were positioned at 45° angles. We also added several black baffles between the lights and the camera to reduce optical flare. The color targets are shown in Figure 17 and described in Table III.

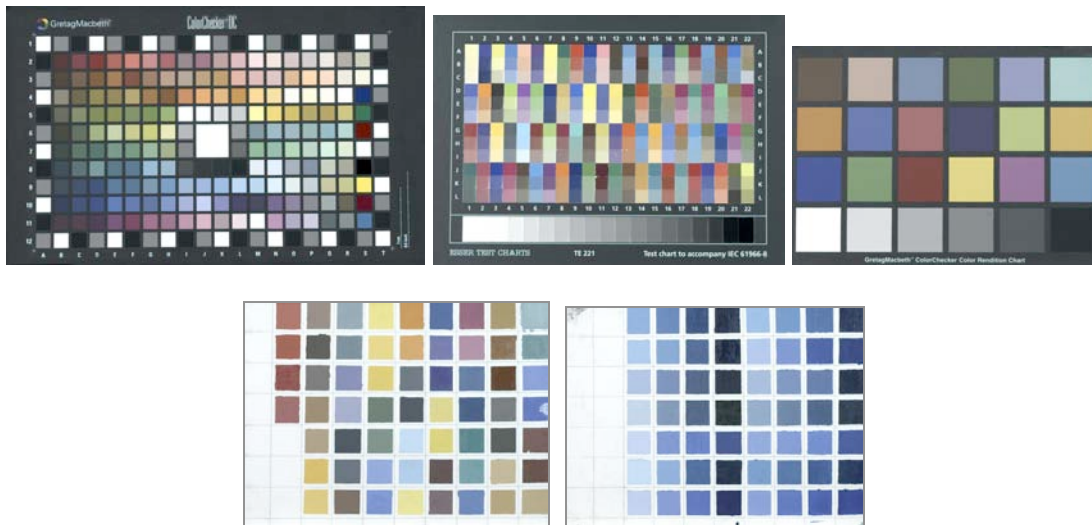


**Figure 17.** Color targets used in imaging experiment. Top row from left to right: ColorChecker DC, Esser, and ColorChecker. Bottom row: Gamblin and Blues. See Table III for a description of each target.

**Table III.** Color target information.

Color Target Name	Abbreviation	Samples	Description
GretagMacbeth ColorChecker DC	CCDC	240	Commercial color target used for camera calibration.
Esser TE221 Test Chart	Esser	264	Flatbed Scanner calibration chart. Made up of 12 different printing inks.
GretagMacbeth ColorChecker	CC	24	Commercial color calibration target commonly used in museum digital and conventional photography.
Gamblin Conservation Colors	Gamblin	63	Samples of 31 Gamblin Conservation Pigments mixed with Titanium White at two ratios.
Blue Pigment	Blues	56	Mixtures of Phtalo, Ultramarine, Prussian and Cobalt Blue pigments with Titanium White.

The exposure time was adjusted for each filter in order to maximize dynamic range without clipping. Images were collected of gray Color Aid paper and each target. Digital flat fielding was accomplished using the gray paper and Equation (5). This accounted for lighting non-uniformity and sensor fixed pattern noise. Dark correction was not necessary since this step is performed within the camera software environment.

$$D_{corrected} = D_{original} \cdot \text{mean}(D_{flatfield}) / D_{flatfield} \quad (5)$$

The gray samples of the CCDC were used to linearize the camera signals with respect to luminance factor.

Equation (3) was used to derive a transformation matrix that converted the flat-fielded, linearized camera signals to spectral reflectance factor. For set A, six camera signals were transformed to estimated spectral reflectance factor from 380 nm to 750 nm in 10 nm increments. For the BG39 filter, three camera signals were transformed to estimated spectral reflectance factor. The CCDC and Blues targets were used to derive this transformation matrix.

It is important to note that the three-channel transformation matrix is equivalent to deriving a (3 x 3) transformation matrix that transforms linearized camera signals to tristimulus values. Because calculating tristimulus values from reflectance is a linear operation, the identical results occur whether one predicts reflectance or X, Y, and Z.

The Esser, ColorChecker and Gamblin targets were used to independently verify the accuracy of the imaging system. Shown in Table IV is the mean performance comparing the production and modified Sinarback 54. Color accuracy was quantified using the 1976 CIELAB total color difference,  $\Delta E^*_{ab}$ , and the recent CIEDE2000 color difference equation,  $\Delta E_{00}$ . Spectral accuracy was quantified using spectral root-mean-square error, RMS, and two indices of metamerism, MI. The first index evaluated spectral mismatch under incandescent illumination while the second evaluated mismatch under daylight illumination. Both indices have units of  $\Delta E_{00}$ . The modified camera resulted in more than a twofold improvement in color and spectral accuracy.

**Table IV.** Mean performance metrics for three camera configurations and five color targets.

Target	Sinarback 54 H + BG39					Sinarback 54 H + Set A Filters				
	$\Delta E^*_{ab}$	$\Delta E_{00}$	sRMS	MI <sub>001</sub>	MI <sub>002</sub>	$\Delta E^*_{ab}$	$\Delta E_{00}$	sRMS	MI <sub>001</sub>	MI <sub>002</sub>
CCDC	6.24	4.72	4.47	1.24	1.30	2.69	1.75	2.36	1.02	1.22
Blue	4.82	3.72	6.75	1.42	1.61	3.22	1.74	2.01	1.04	0.91
Esser	5.78	3.93	5.80	1.49	1.63	3.30	1.79	2.66	0.91	1.02
Gamblin	6.31	4.29	8.27	1.37	1.67	3.41	2.10	3.32	0.68	0.88
CC	6.33	4.58	6.75	1.54	1.53	3.40	1.93	2.93	0.89	1.03

Bar graphs comparing spectral and colorimetric performance are shown in Figures 18 and 19. The modified camera system had excellent performance, particularly given it is a CFA camera whose spectral properties are fixed.

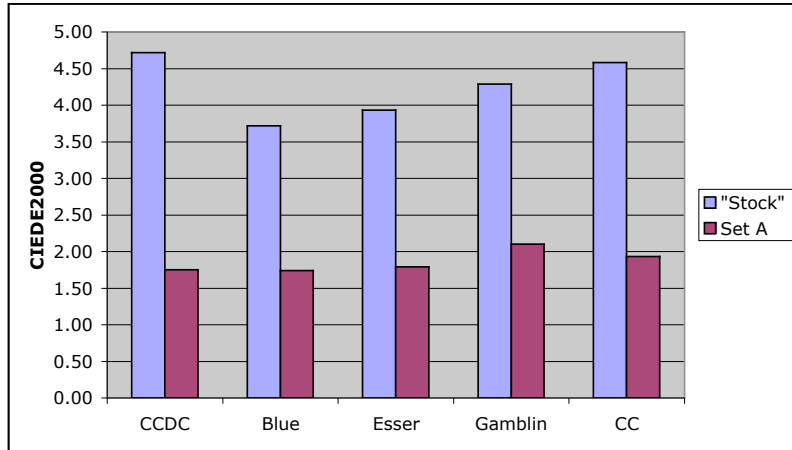


Figure 18. Color accuracy comparison using data shown in Table IV.

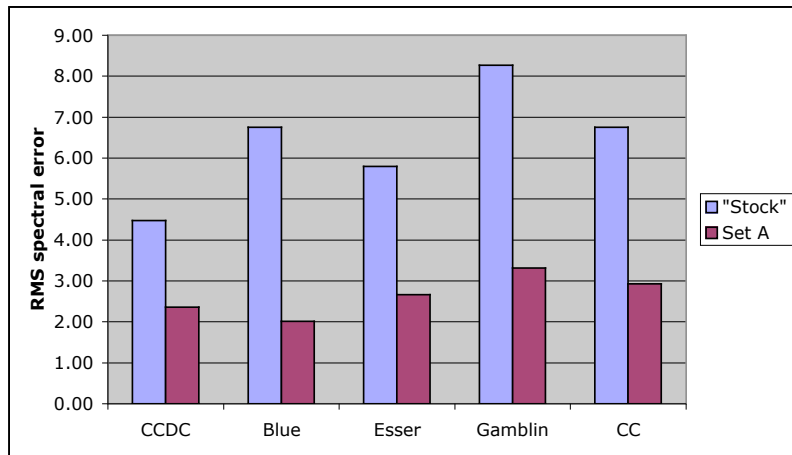
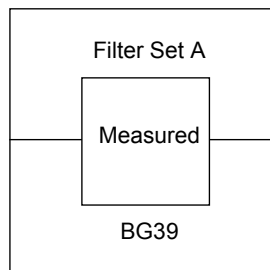
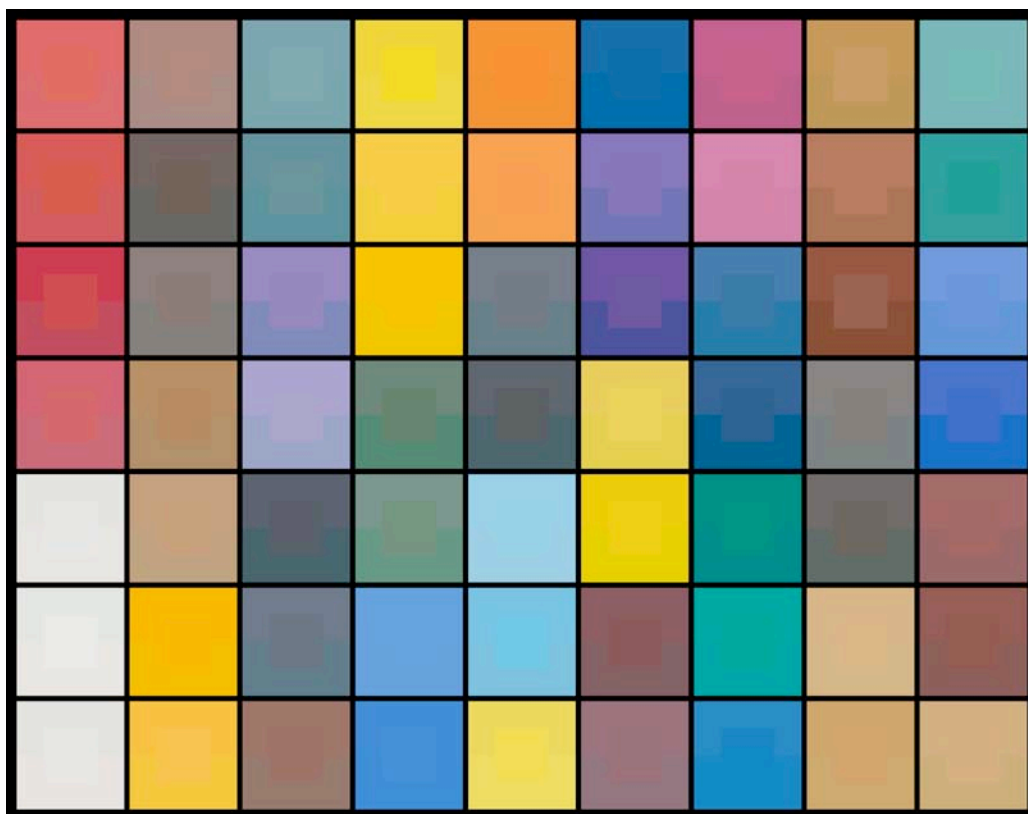
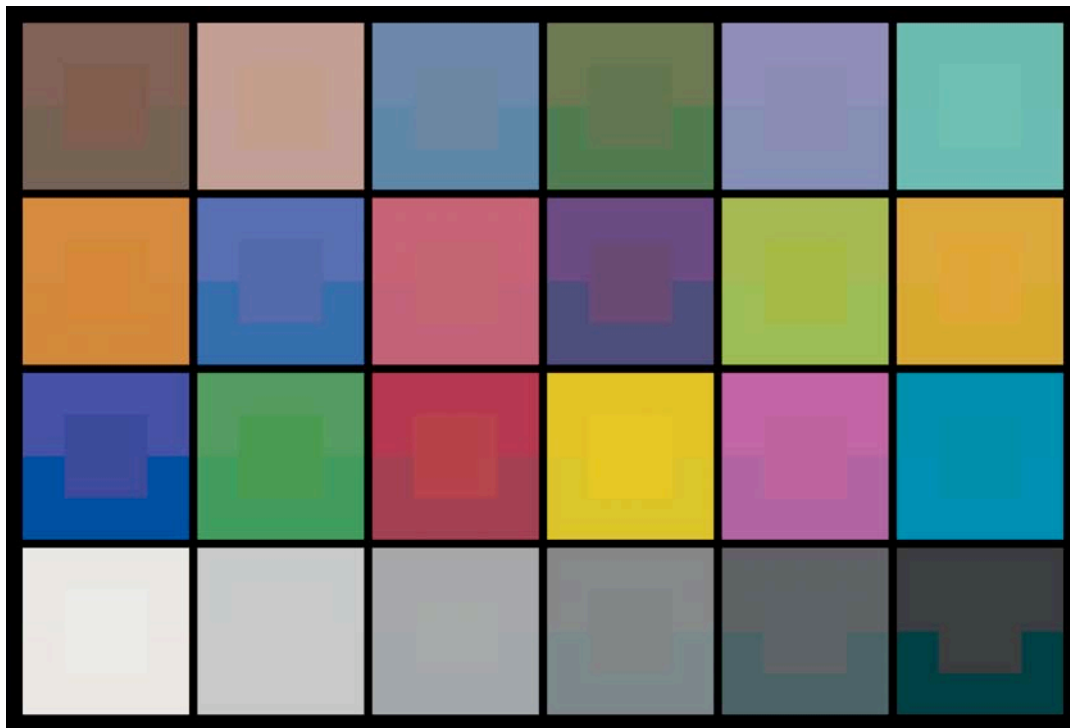


Figure 19. Spectral accuracy comparison using data shown in Table IV.

The improvement in colorimetric accuracy using the original Sinar camera and its modification using Filter set A can also be visualized by rendering what the color targets would look like under a particular illuminant. In Figure 20, the center of each square is rendered for D65 using the color calculated from direct spectral measurements of the target. The top portions of the squares are rendered using the images taken through filters set A and the spectral estimation method described above. The bottom portion of the squares are rendered using the BG39 filtered images and the same estimation technique. The better the filters and spectral estimation method the closer the color will match between the edge sections and the middle.





**Figure 20.** Color targets rendered for D65 and the 1931 standard observer using spectral estimation and direct measurements. For each color sample, the middle is from direct measurements, the top from filter set A and the bottom from the BG39 images. The upper target is the Color Checker; the bottom target is the Gamblin conservation colors.

The transformation matrix estimates spectral reflectance from camera signals. The estimated spectra from the modified camera using filter set A are shown in Figure 21 for the Color Checker. In general, the spectral features are estimated reasonably. There is greater spectral variability in the estimated spectra; this is seen in the white sample (bottom left). The estimated spectra using the “stock” Sinarback 54 are plotted in Figure 22. For some samples, there are significant errors, particularly at long wavelengths where reflectance is under-predicted. Estimated spectra for the Gamblin target are shown in Figures 23 and 24. The same trends are evident.

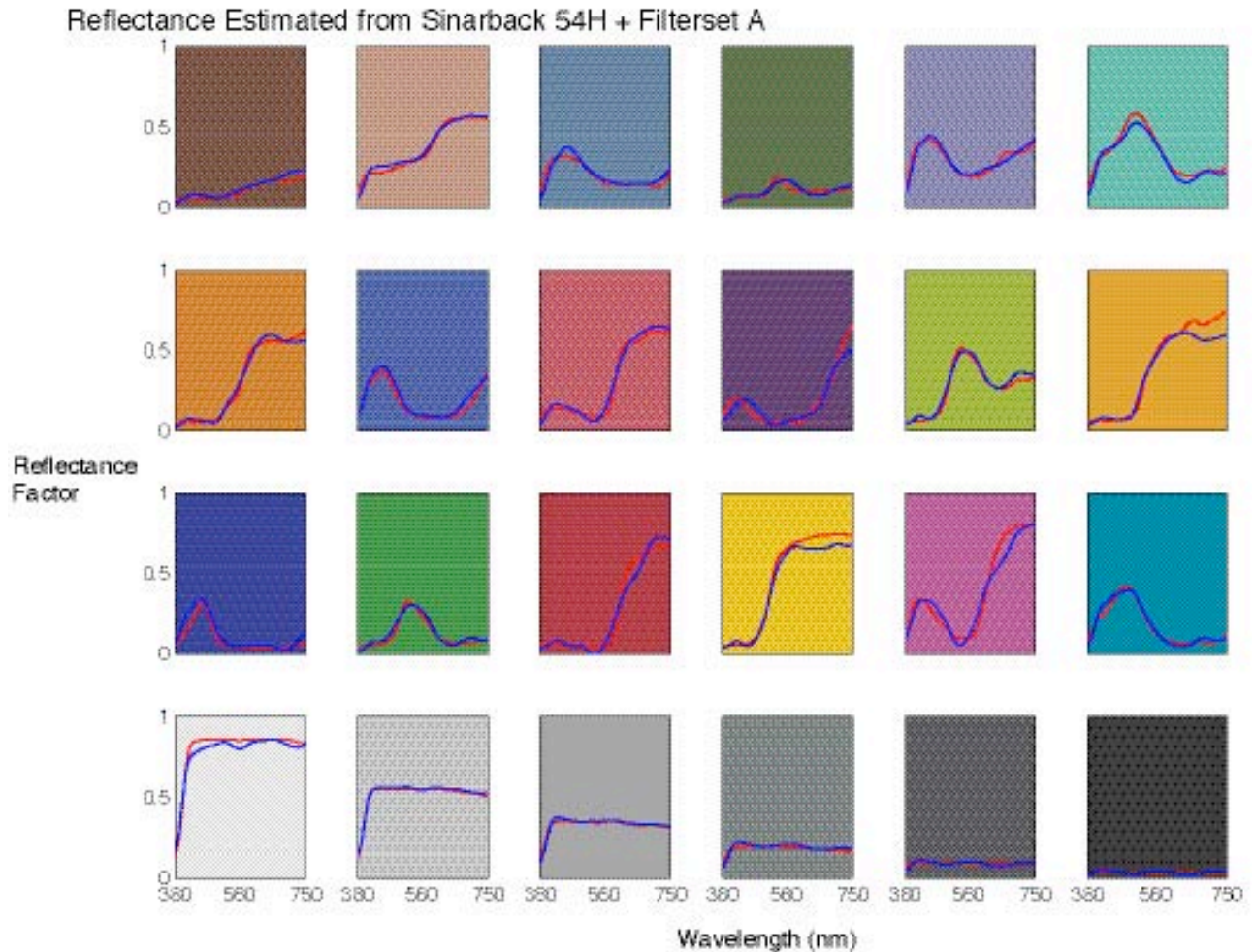


**Figure 21.** Direct measurements (red lines) and imaging spectral estimates (blue lines) for the Color Checker reflectance spectra using filter set A modified Sinarback 54.

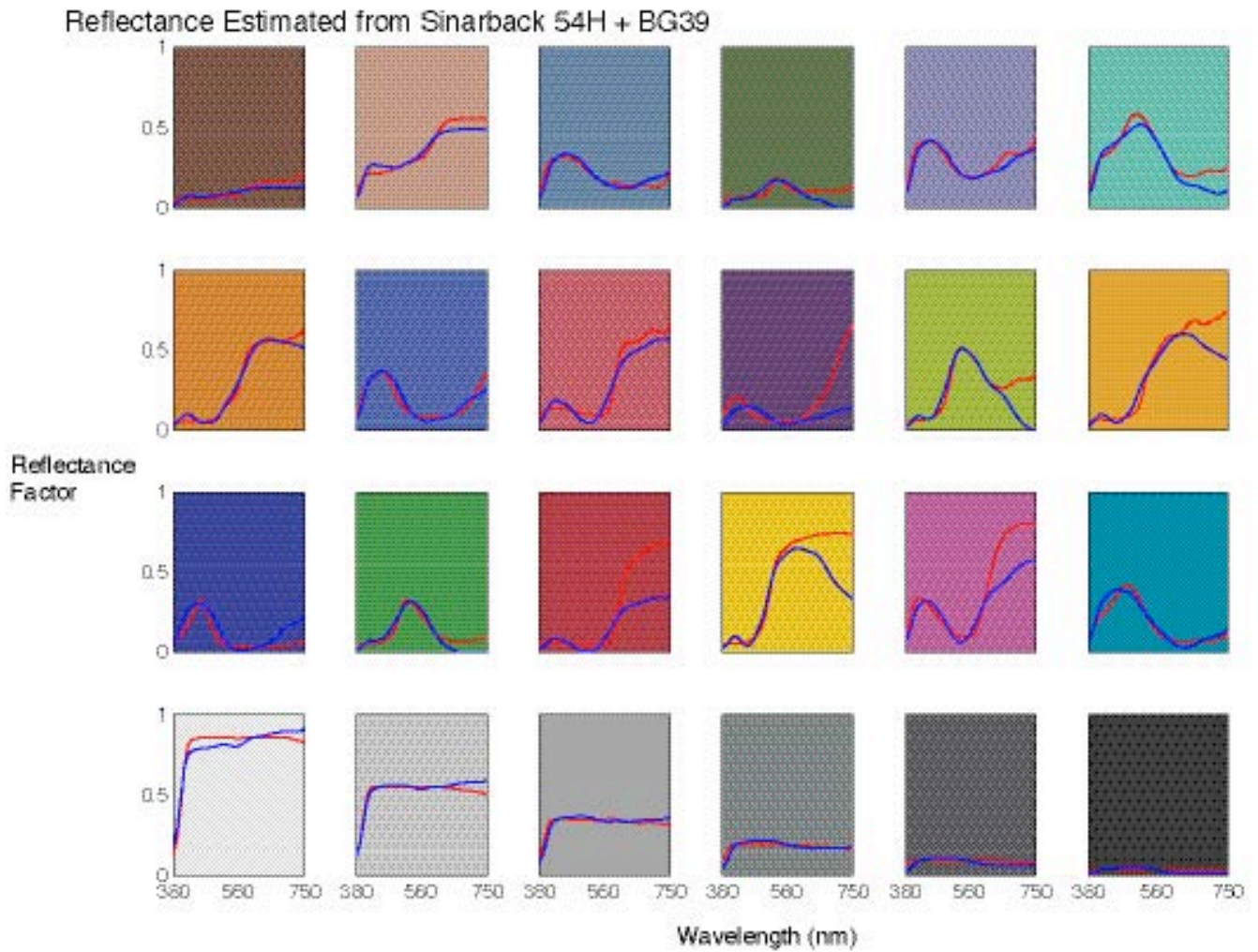


**Figure 22.** Direct measurements (red lines) and imaging spectral estimates (blue lines) for the Color Checker reflectance spectra using the “stock” Sinarback 54.

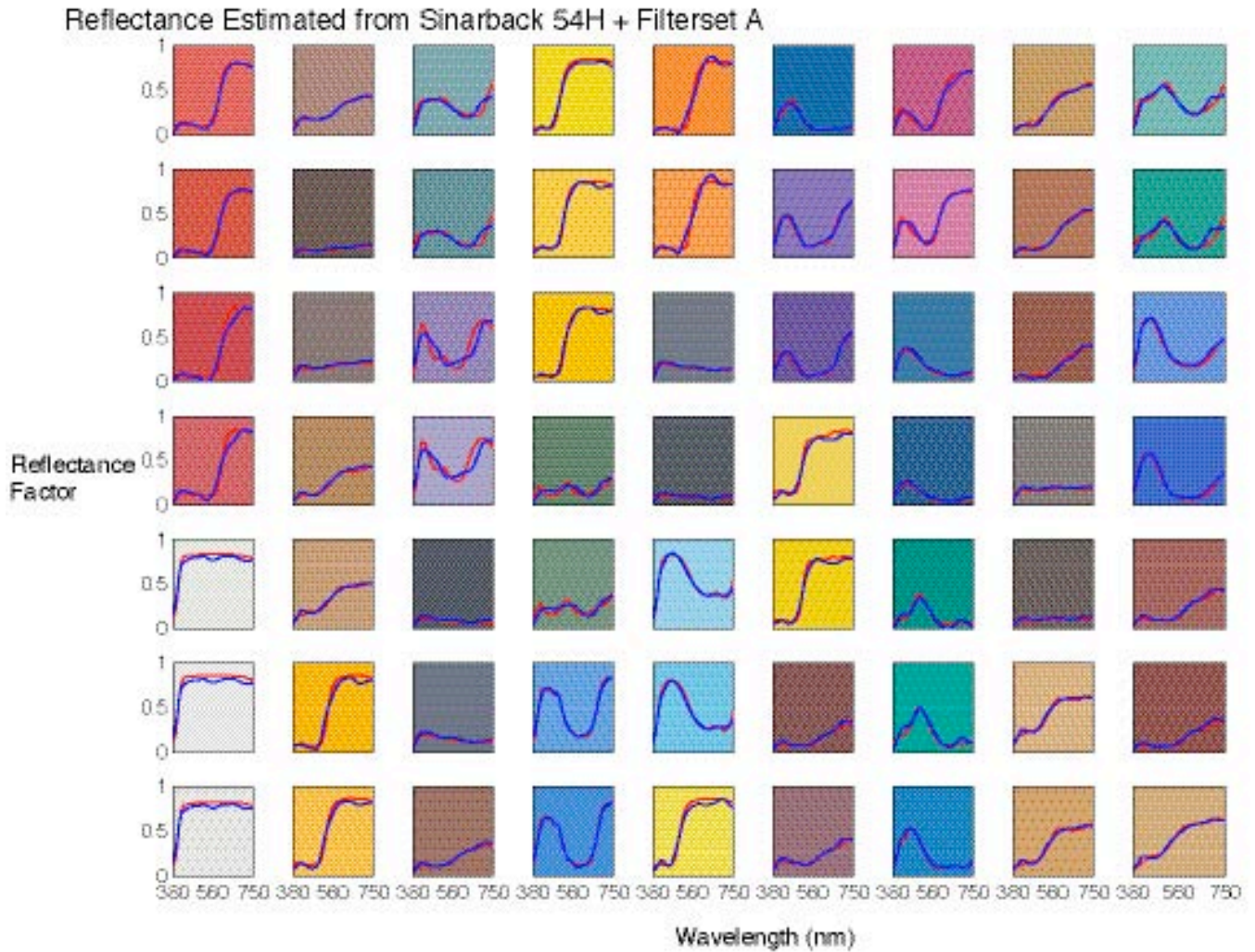


**Figure 23.** Direct measurements (red lines) and imaging spectral estimates (blue lines) for the Gamblin Conservation Colors reflectance spectra using filter set A modified Sinarback 54.

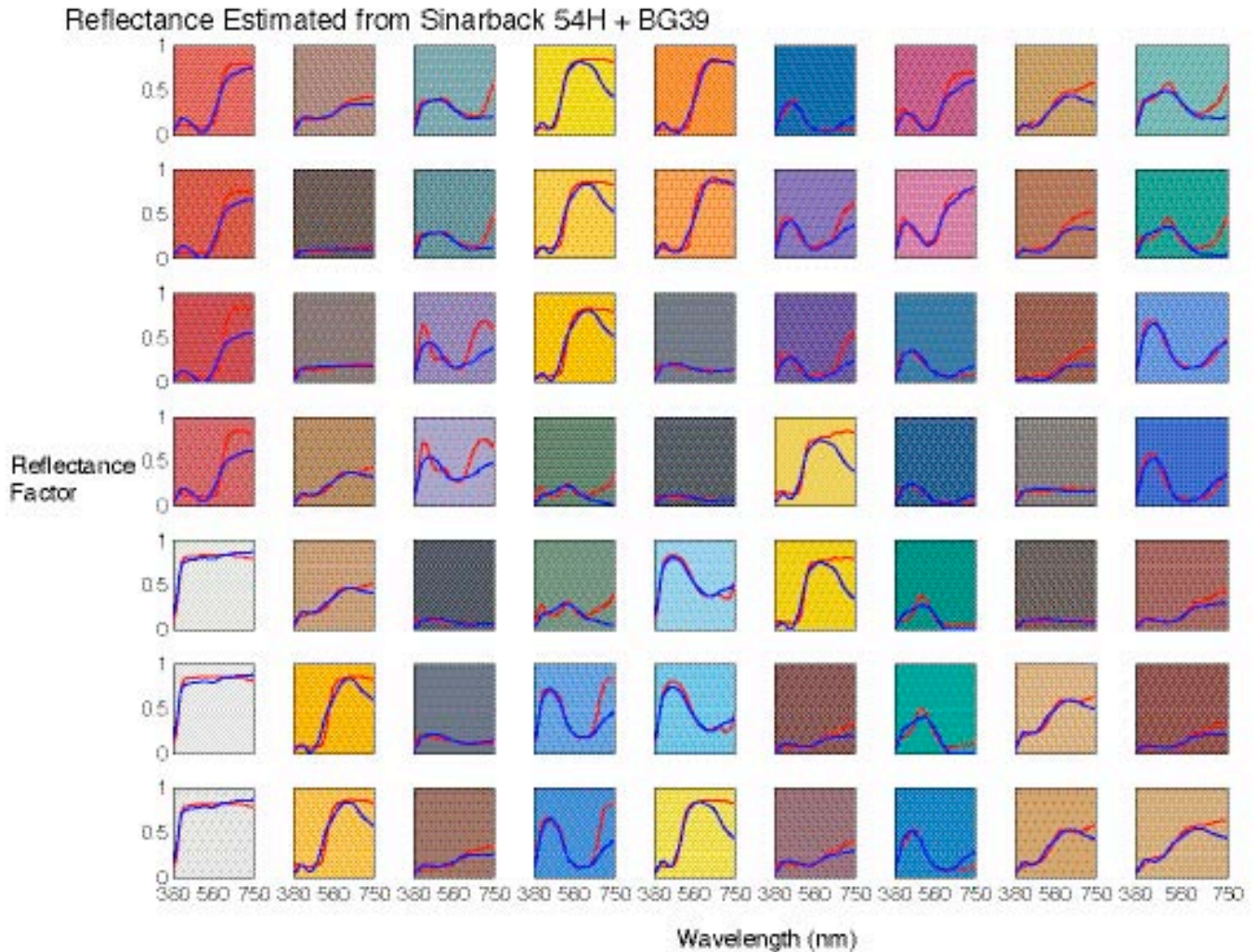


**Figure 24.** Direct measurements (red lines) and imaging spectral estimates (blue lines) for the Gamblin Conservation Colors reflectance spectra using the “stock” Sinarback 54.

### XIII. Conclusions

The multi-filter approach was very effective in improving the colorimetric accuracy of a production CFA digital camera. This provides a practical method to achieve accurate color images and a reasonable spectral archive.

Future research will evaluate more elaborate mathematical techniques of spectral estimation, further optimizations that will identify a filter set with increased throughput, and the influence of the camera-taking illuminant on performance.

### IX. References

1. See [www.art-si.org](http://www.art-si.org).
2. S. Quan, Evaluation and Optimal Design of Spectral Sensitivities for Digital Color Imaging, Ph.D. Dssertation, R.I.T., Rochester, NY, 2002.

## X. Appendix: Comparison of Experimental and Computational Results

The experiment of imaging the five target described above was carried out for two reasons. The first was to test how well the selected filters performed under real conditions outside the simulation. The second purpose was to verify the accuracy of the theoretical camera model used to perform the filter selection.

To make the comparison between the measured camera output and the model predictions it was necessary to perform the spatial correction described in Equation (5) because the model assumes uniform lighting. Figure A1 shows the measured versus simulated output of the camera for the CCDC target using filter set A combined with Unaxis IR cut-off filter and the HMI lighting. There are high correlations between measured and calculated digital counts for all six channels, (0.9897, 0.9952, 0.9940, 0.9953, 0.9797, and 0.9922), for channels one through six respectively. Channel five has lower correlation than the others, which is also seen in Figure A1 where the points are more scattered. This channel only lets through near infrared energy and may not be responding to in a completely linear fashion with the amount of light as the model assumes.

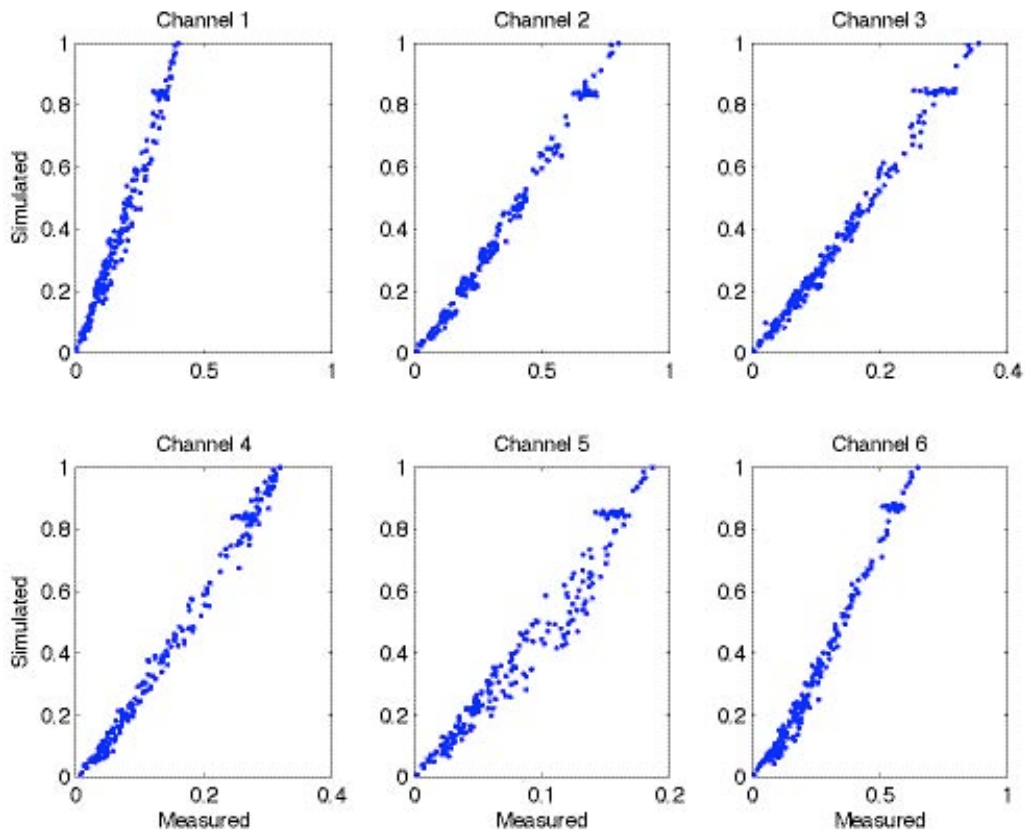


**Figure A1.** Calculated digital counts based simulation versus measured digital count for a simulated system using measured camera sensitivity, Unaxis IR cut-off filter, HMI lighting, and filter set A.